DESIGN IMPROVEMENT BASED ON WEAR OF A JOURNAL BEARING USING AN ELASTOHYDRODYNAMIC LUBRICATION MODEL

Mustafa DUYAR[1], Zafer DURSUNKAYA[2]

[1]Ricardo Software,
Prague, Czech Republic
Phone: 420 221 729 150, Fax: 420 221 729 195,
E-mail: mustafa.duyar@ricardo.com

[2]Middle East Technical University, Mechanical Engineering Department,
Ankara, Turkey
Phone: 90 312 210 5232, Fax: 90 312 210 1266,
E-mail: refaz@metu.edu.tr

ABSTRACT

In the design analysis of journal bearings, reduction of wear is important as operating conditions may lead to scoring, scuffing or seizure at the pin bearing, which affects performance, efficiency and reliability of the component negatively. In this study, a model of elastohydrodynamic lubrication of a journal bearing is used along with the simulation of the slider-crank mechanism of motion, to study the effect of design parameters on computed wear on the bearing surfaces. Calculated asperity contact pressure in the boundary lubrication model is used to predict wear rate by Archard law. The model is used to analyze the lubrication of the connecting rod small end bearing of a reciprocating hermetic compressor, and bearing parameters are changed to reach a better design in terms of reduced wear.

1. INTRODUCTION

Journal bearings are used in numerous applications in diverse machinery. The design of journal bearings has long been based on the rigid hydrodynamic analysis of the components. The elastohydrodynamic lubrication (EHL) approach is given by Dowson and Higginson, [1]; Hamrock and Dowson, [2]; and Gohar [3], and it accurately predicts the profile and thickness of the lubricating film. The use of EHL approach in the design has, therefore resulted in an improvement in the design and as a result in the working performance and durability of bearings. In this lubrication regime, hydrodynamic pressures are sufficiently high that a significant elastic deformation of the interacting surfaces is caused. The use of EHL approach shows that the film thickness is slightly influenced by the elastic moduli of the surfaces. The EHL analysis of connecting rods has been of considerable interest in the recent past. Implementations of improved fixed point EHL-iteration schemes were presented by LaBouff and Booker [4] as well as by Fantino and Frene [5]. Oh and Goenka [6] presented a stable and fast Newton-Raphson scheme and a solution. Van der Tempel et al. [7, 8] combined Newton-Raphson and inverse hydrodynamic methods, an approach that is very well suited for highly compliant bearing structures. Kumar et al. [9] introduced modal reduction techniques for faster solutions in the context of quasi-static deformation analysis, an attribute that holds for all the above references. Dursunkaya et al. [10] solved the EHL problem of a piston in the context of the analysis of secondary dynamics of piston components. Duyar and Dursunkaya [11] addressed the problem of design improvement based on the minimization of boundary contact forces between the two surfaces.

In the current study, the model for the EHL analysis of a journal bearing and wear of the bearing surfaces is developed. The approach is exercised for the design improvement of the wristpin-small end bearing of a reciprocating hermetic compressor, ARÇELİK TE165. Slider-crank dynamics is solved to provide dynamics data for the lubrication problem, where, wrist-pin elastohydrodynamic and boundary lubrication, and elastic deformations are simultaneously solved. Resulting boundary contact pressures are used to obtain wear rate predictions. Design parameters are altered to reach a superior design in terms of reduced wear.

2. MODELLING

In this study a computer code that can be used for the elastohydrodynamic analysis of a journal bearing is developed, and is applied to the design improvement of a compressor wristpin-connecting rod small end bearing. The approach used by Duyar and Dursunkaya [11] is applied to the current problem. The comparison between a rigid *vs*. elastic modeling and the validity of the basic predictions of the current approach are studied in [11]. Slider-crank dynamics are solved to provide dynamics data for the lubrication problem, and the wristpin elastohydrodynamic and boundary lubrication, and elastic deformations are simultaneously solved for the hydrodynamic and contact pressures and pin deformations. The wear rates of the wristpin and connecting rod small end bearing surfaces are predicted by using the Archard law for wear. The deformations are calculated using the wristpin compliance matrix derived from a finite element model of the wristpin.

2.1 Wristpin Elastohydrodynamic Lubrication

The equations governing the wristpin EHL problem are the Reynolds equation for the pressure distribution and the elasticity relationships for wristpin deformation. The Reynolds equation:

$$\frac{\partial}{\partial z}\left(h^3\frac{\partial P}{\partial z}\right)+\frac{1}{R^2}\frac{\partial}{\partial \theta}\left(h^3\frac{\partial P}{\partial \theta}\right)=6\mu\omega R\frac{\partial h}{\partial \theta}+12\mu\frac{\partial h}{\partial t}, \tag{1}$$

relates the hydrodynamic pressure to the film thickness. In this equation, the dependent variables P and h denote the hydrodynamic pressure and film thickness, respectively. The axial coordinate z, the circumferential direction θ and time t, are the independent variables. The parameters μ, ω and R denote the dynamic viscosity, relative rotational speed and the radius of the shaft, respectively. The film thickness includes the effect of connecting rod motions, bearing clearance and elastic deformation. In the current approach, only radial deformations on the bearing surface of the wristpin are considered. Other (*i.e.* axial, tangential) deformations are comparatively small and do not affect the film thickness. The elastic relationship relating radial deformations on these surfaces to the applied hydrodynamic and boundary pressure is given by,

$$\delta(z,\theta,t)=\mathbf{C}\cdot(P+P_c), \tag{2}$$

where δ is the radial deformation of the shaft and P_c is the boundary contact pressure. The compliance matrix $\mathbf{C}$ is corrected to include the effect of the area and, therefore, the nodal radial deformations are linearly related to nodal pressures. The distributions of wrist-pin elastic deformation δ and the film thickness h are related to each other by,

$$h(z,\theta,t)=h_{dyn}(z,\theta,t)+\delta(z,\theta,t). \tag{3}$$

In case of a hermetic compressor, the pressure inside the hermetically sealed shell is equal to suction pressure, resulting in the following boundary conditions in the axial direction,

$$P=P_{sc}, \quad z=0,L, \tag{4}$$

where L is the length of the bearing. In the cavitating region, half Sommerfeld condition is assumed to be valid, therefore,

$$P=P_{sc}, \text{ if } P<P_{sc}. \tag{5}$$

Due to the small clearances encountered in the analyzed applications, the possibility of boundary contact must be accounted for, since hydrodynamic pressures may not be sufficient to prevent solid-to-solid contact. For bearing surfaces in close proximity, a model for contact pressures between two nominally flat surfaces given by Greenwood and Trip, [12] is used. The model has a statistical representation of surface roughness, which uses three roughness parameters, and is used to calculate the effective asperity contact pressure at each point of the EHL mesh.

For the formulation and solution of the elastohydrodynamic lubrication problem, the approach of [10] is used. The Reynolds equation is discretized, and when combined with the deformation relation given in Eq. (3) and the clearance given in Eq. (4), this resulted in a coupled set of equations for the clearance, h, deformation, δ, and the hydrodynamic pressure P. As the boundary pressure P_c is a function of clearance only, knowledge of the clearance enables the computation of boundary contact pressures. The equations are solved in an iterative manner as follows:

1. At every time step an estimate of the journal orbit is made to simultaneously solve for pressures and deformations, iteratively, until convergence. This is repeated for every perturbation of the Newton-Raphson scheme used in the solution of the force balance.
2. Resulting forces are obtained *via* integration of boundary and hydrodynamic pressures. The force balance on the pin is solved using a Newton-Raphson scheme iteratively, until convergence.
3. The solution is advanced in time to solve for the next time step.

To ensure the cyclic convergence of the results, the entire problem is solved typically for 5-7 cycles, after which results are cyclically repeating.

2.2 Wear Model

With the knowledge of contact pressures and the surface velocities, the wear rate on the wristpin and connecting rod small end bearing surfaces can be generated by using Archard law [13,14], given as

$$W_r = k\frac{W \cdot V}{H}, \tag{6}$$

where W_r is the wear rate, W is the applied load, H is the hardness of the sliding material, V is the sliding speed, and k is a constant, referred to as the wear coefficient. In the current problem the applied load on the journal, as well as the sliding velocity is time dependent, therefore using the Archard law instantaneously, and averaging over the cycle gives the cycle averaged wear rate, $W_{r,av}$ as,

$$W_{r,av} = \frac{k}{H}\frac{1}{T}\int_0^T W_L\,dt = \frac{k}{H}\frac{1}{T}\int_0^T\int_A P_c|V|\,dA\,dt, \tag{7}$$

where V is the sliding velocity of the connecting rod small end, T is the period of the compressor cycle and W_L is the wear load.

The wear coefficient, which is an input to the program, is not easily obtained and is a function of several variables including lubrication conditions, lubricity, and sliding velocity. In the current study, a single value for the wear coefficient is used for all velocities, although the sliding velocity is time dependent.

2.3 Compliance matrix, finite element (FE) model

To compute the radial deformations on the wristpin surface, the compliance matrix used in the EHL calculation is extracted using a commercial FE code, from a FE model of the pin. In this analysis, the connecting rod is considered rigid and the wristpin elastic. The FE code is used to obtain –*via* a substructure analysis– the stiffness matrix of the pin surface and a pre-processing program inverts the stiffness matrix to obtain the compliance matrix to be used in the EHL analysis. The stiffness/compliance matrices are generated for the radial degrees of freedom on the surface of wristpin. In the elastic problem, the nodes contacting the piston pin hole were restrained.

3. RESULTS AND DISCUSSION

The physical dimensions and pressure data of a compressor running at ASHREA rating conditions, pertaining to a production of Arçelik TE165 compressor are used in this parametric study. Simulations are run until cyclical convergence is achieved, typically in 5 cycles. When the lubricant viscosity is increased, the number of cycles to reach convergence increases to seven. In the parametric study the effect on wear of design and operating parameters, that could be altered, are analyzed. In this context, the lubricant temperature, nominal clearance, pin material, journal diameter and bearing length are chosen as the parameters that could be changed. The results of the parametric runs are analyzed to reach an “optimum” solution, with the aim of a reduction of boundary contact, and consequently, projected wear.

3.1 Effect of Lubricant Temperature

The effect of lubricant temperature on the performance is studied, since it directly affects the lubricant viscosity. In case of the baseline operation, the fluid is at 100°C, the temperature encountered in compressor operation, and the other cases are exercised for fluid at 75°C, 50°C and 25°C, corresponding to cooled refrigerant. Fig. 1 shows the effect of temperature variation on the orbital motion inside the bearing and the radial deformation of the pin. With a

decrease in temperature, and corresponding increase in lubricant viscosity, the motion of the pin inside the sleeve slows down. With reduced viscosity, the pin moves inside the sleeve under the effect of the cyclically varying load, and an increase in viscosity keeps the pin at a relatively less varying distance from the sleeve. As far as the boundary contact and the resulting wear are concerned, this has two contradictory consequences. The pin comes to a closer proximity of the sleeve near TDC, when the load is at a maximum in the case when the viscosity is low, thus increasing the boundary contact. The pin assumes a more centered position elsewhere during the cycle, reducing boundary contact. When the boundary contact forces in the axial direction are viewed in Fig. 2, this effect can be seen. The change in lubricant temperature was not seen to affect the deformations considerably (Fig. 1). The baseline case results in large boundary forces near TDC, elsewhere the boundary forces are small. With an increased viscosity, the contact phenomenon near TDC eases, but at other locations the magnitude of boundary forces are more elevated compared to the baseline case. As the lubricant temperature decreases, the cycle averaged wear rate also decreases. Although with an increased viscosity, the contact phenomenon near TDC eases, at other locations the magnitude of boundary forces are more elevated compared to the baseline case. This increase all through the cycle, except near TDC, is smaller compared to the decrease near TDC, and the cycle averaged wear rate get smaller with increased viscosity up to 50°C. Due to this effect, the cycle averaged wear rate in 25°C is more than in 50°C. The result of this on the cycle averaged wear rate is given in Fig. 3.

The predicted location of wear on the wristpin and connecting rod small end for baseline simulation were in seen to be in agreement with wear locations and patterns seen in compressor tests. Region subjected to wear on the connecting rod small end is located where the line of centers of big end and small end pass. The wear patterns are predicted and observed at the corresponding location on the wristpin.

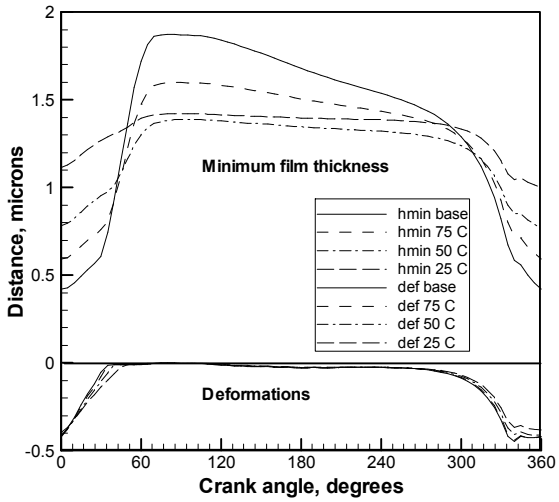

Figure 1. Effect of lubricant temperature on minimum film thickness and maximum deformation

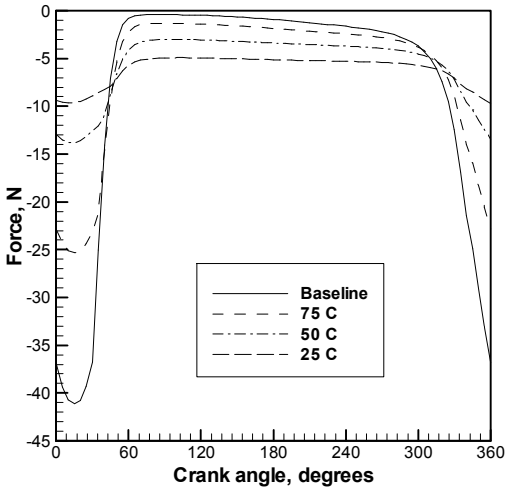

Figure 2. Effect of lubricant temperature on boundary contact forces

3.2 Effect of Nominal Clearance

To study the effect of bearing clearance on performance, simulations are carried out for various connecting rod-pin nominal radial clearances. For the baseline case, the radial clearance was 4 μm, and the other cases are run for clearances of 3.5, 5, 6, 7, and 8 μm. An analysis of the results shows that a decrease in clearance keeps the pin at a relatively less varying distance from the sleeve. When the boundary contact and the resulting wear are concerned, two contradictory consequences occur, similar to the viscosity sweep case. It is observed that a reduction in nominal clearance reduces the boundary contact force occurring near the TDC, however, elsewhere in the cycle there occurs a prolonged but diminished – in magnitude – boundary contact. An increase in the nominal clearance has just the opposite effect. The clearance alteration does not affect the deformations.

When the cycle averaged wear rates are examined in Fig. 4, it can be seen that the minimum wear rate occurs at the

nominal clearance of 5μm. Although, the nominal clearance of 3.5μm has the smallest boundary contact force near TDC, its magnitude is elevated at other crank angles during the cycle.

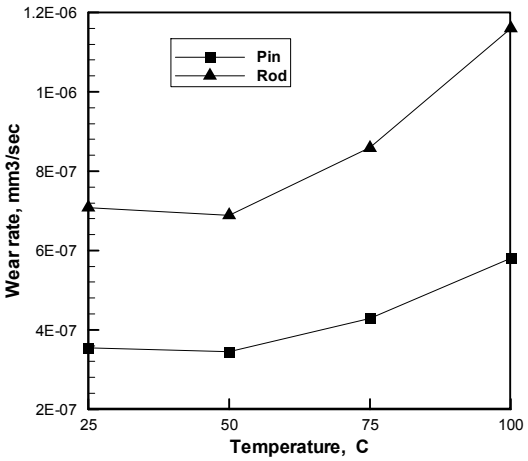

Figure 3. Effect of lubricant temperature on cycle averaged wear rate

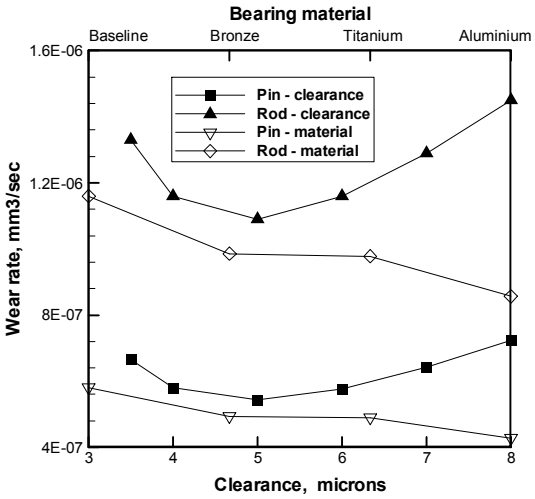

Figure 4. Effect of nominal clearance and pin material on cycle averaged wear rate

3.3 Effect of Pin Material

Engineering materials, which can be considered as alternatives to the currently used baseline wristpin material are investigated without any consideration of strength, fatigue and cost. Aluminum alloy, bronze and titanium material properties are used in this set of simulations. The aluminum alloy has the minimum elastic modulus among the materials and this case results in the best conformity of the connecting rod and pin, resulting in maximum deformations. Baseline material is stiffer than the others; therefore the deformations are observed to be smaller. Although the minimum film thickness seen in case of aluminum is the smallest of the four, due to larger deformations it conforms better to the shape of the journal and a reduction in boundary contact force is realized throughout the cycle. The cycle averaged wear rates are given in Fig 4. As the elastic modulus of the wristpin material decreases, it conforms better to the shape with diminished boundary contact and reduces the wear rate. Due to better conformity, cycle averaged wear rate has the smallest value for the aluminum alloy wristpin.

3.4 Effect of Bearing Diameter

The pin diameter affects the bearing performance, since an increase in diameter increases the bearing area. For the baseline case, the wristpin is 7.9324 mm in diameter. Simulations are performed by increasing the baseline value by 10% and 20%, resulting in an increase in the hydrodynamic pressure acting area. The simulations show that increasing the bearing diameter increases the minimum film thickness and results in up to 20% reduction in peak boundary contact forces. Increasing the bearing diameter results in increased bearing area; and although the contact forces decrease with increased diameter, contact forces acting area also increases, and the wear rates do not change considerably. The wear rate predictions for various bearing diameters are given in Fig. 5.

3.5 Effect of Bearing Length

A change in bearing length directly affects the bearing performance. In an existing design, however, such a change is hard to accomplish. In the current study the bearing length of the existing design is 8 mm. Two other cases are investigated, where the length is increased to 10 and 16mm. Increasing the length to 10 mm is practically possible, however, due to piston geometry of the design in question; using a 16 mm bearing length is not feasible. The parametric study was, nevertheless conducted, in order to assess the affect of an increase in bearing length on wear. Using longer bearings increased the bearing area, as a consequence the hydrodynamic pressure acting area, and the minimum clearances around TDC increases, resulting in a decrease in boundary contact force. The boundary contact forces near TDC decreased with the increase in bearing length but at other crank angles of the cycle they are

elevated. In addition, a similar effect as the case of diameter increase is observed, the contact area increases, therefore volumetric wear rate is higher than the baseline case. In other words, by increasing the bearing length the hydrodynamic force acting area increases, so does the wear area and for the 16 mm bearing length, cycle averaged wear rate increases from 5.795×10^{-7}mm³/s to 6.507×10^{-7}mm³/s for wristpin and 1.160×10^{-7}mm³/s to 1.303×10^{-7}mm³/s for connecting rod small end. The wear rate results are given in Fig. 5.

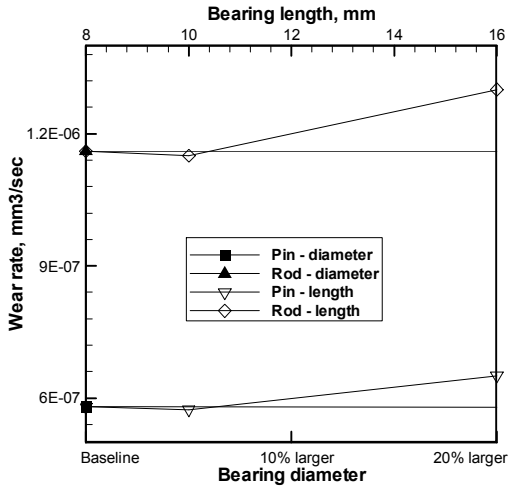

Figure 5 Effect of bearing diameter and length on cycle averaged wear rate

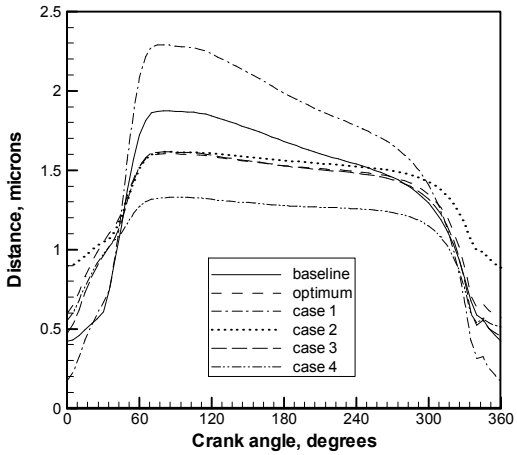

Figure 6 Minimum film thickness for improved cases

Table 1 Baseline and altered parameters

Case	Temperature (^{o}C)	Material	Diameter	Clearance (μm)
Baseline	100	Steel	7.9324 mm	4
Optimum	50	Aluminum	10% increased	5
Case1	100	Aluminum	10% increased	5
Case 2	50	Steel	10% increased	5
Case 3	50	Aluminum	7.9324 mm	5
Case 4	50	Aluminum	10% increased	4

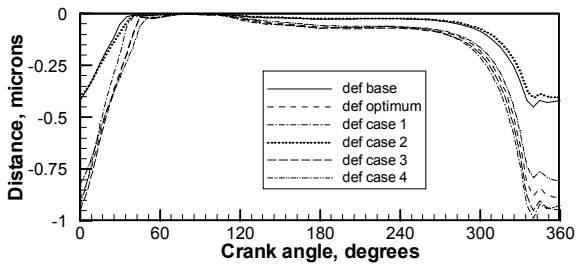

Figure 7 Maximum deformation for improved cases

3.6 Design Improvement

To arrive at an improved design with reduced wear, the results of the above parametric study are used to generate a set of alternative designs. In this analysis, a comparatively better design alternative is sought by using the results of the above parametric study. Initially the parameters leading to the best wear characteristics are chosen to designate an "optimum" case. Afterwards by changing one parameter at a time to the original value, four alternative designs are suggested for analysis. Table 1. summarizes the parameters used in this study. A comparison of the baseline

and optimum cases in Figs. 6, 7 and 8 show that although minimum clearance around TDC does not change considerably, the deformation levels are higher in the optimized cases, and the pin conforms better, as a result of which the boundary contact force decreases from approximately 40 N to 7 N. Similarly, cycle averaged wear rates decrease to approximately one third of the baseline case as shown in Fig. 9. All cases demonstrate improvement in the wear, and practically Case1 is the easiest to implement on the existing design, and is observed to reduce the wear rate by approximately 50%. Using a steel wristpin instead of aluminum, as in Case2, increases the wear rate by approximately 35%. If the wear rates of the "optimum" and Case3 are compared, it is possible to conclude that 10 percent diameter increase need not be implemented, since they both give almost identical wear rates. Case4, with the 4 μm –baseline– clearance, increases the wear rate by 80% compared to the 5 μm clearance, which the "optimum" case has.

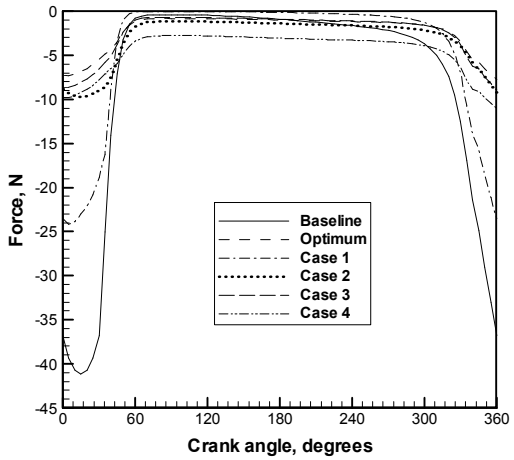

Figure 8 Boundary contact forces for optimized cases

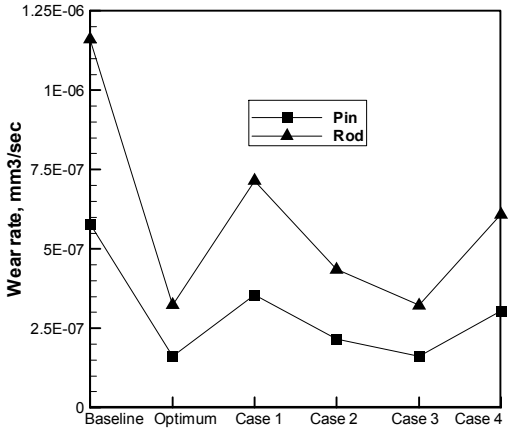

Figure 9 Cycle averaged wear rates for optimized cases

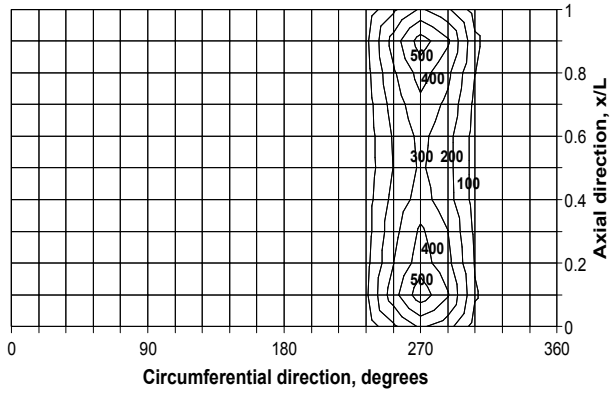

Figure 10 Accumulated wear rate of wristpin on the lubricated portion for the baseline case, $mm^3/s \times 10^{12}$

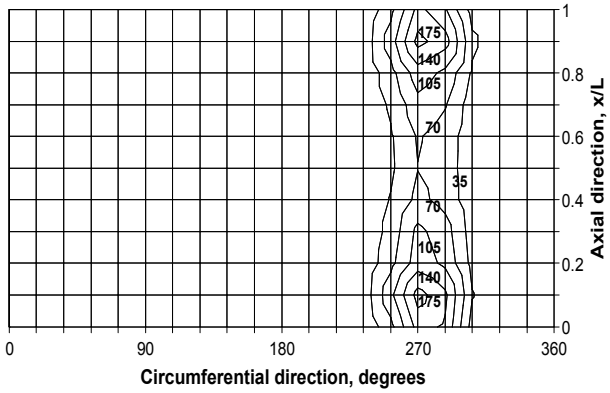

Figure 11 Accumulated wear rate of wristpin on the lubricated portion for the "optimum" case, $mm^3/s \times 10^{12}$

Accumulated wear rate contours of the wristpin for the baseline and the optimum cases are given in Figs. 10 and 11, respectively. Similar to the cycle averaged wear rates, the wear rates decrease in magnitude to approximately one third for both wristpin and connecting rod small end. The location of wear is not affected.

4. CONCLUSIONS

An elastohydrodynamic lubrication model is developed and used along with Archard law to predict wear rate. To the purpose of reduction in wear the effects of lowering the lubricant temperature, increasing the journal diameter, using a more conforming material to improve conformance, changing the bearing length and clearance are investigated. Predictions show that using a more conforming bearing material and cooling the lubricant to increase its viscosity would result in comparatively better design. It should also be mentioned that an analysis that accounts for the elasticity of the connecting rod should produce a more realistic simulation of the underlying physical phenomena.

REFERENCES

[1] Dowson, D., and Higginson, G. R., 1966, "*Elastohydrodynamic Lubrication*," Pergamon

[2] Hamrock, B. J., and Dowson, D., 1981, "*Ball Bearing Lubrication*," John Wiley & Sons

[3] Gohar, R., 1988, "*Elastohydrodynamics*," Ellis Horwood

[4] LaBouff, G., and Booker, J. F., 1985, "*Dynamically Loaded Journal Bearings: A Finite Element Treatment for Rigid and Elastic Surfaces*," ASME Journal of Tribology, **107**, pp 505-515

[5] Fantino, B., and Frene, J., 1985, "*Comparision of Dynamic Behaviour of Elastic Connecting-Rod Bearing in Both Petrol and Diesel Engines*," ASME Journal of Tribology, **107**, pp. 87-91

[6] Oh, K. P., and Goenka, P. K., 1985, "*The Elastohydrodynamic Solution of Journal Bearings Under Dynamic Loading*," ASME Journal of Tribology, **107**, pp. 389-395

[7] van der Tempel, L., Moes, H., and Bosma, R., 1985, "*Starvation in Dynamically Loaded Flexible Short Journal Bearings*," ASME Journal of Tribology, **107**, pp. 516-521

[8] van der Tempel, L., Moes, H., and Bosma, R., 1985, "*Numerical Simulation of Dynamically Loaded Flexible Short Journal Bearings*," ASME Journal of Tribology, **107**, pp. 396-401

[9] Kumar, A., Booker, J. F., and Goenka, P. K., 1990, "*Modal Analysis of Elastohydrodynamic Lubrication: A Connecting Rod Application*," ASME Journal of Tribology, **112**, pp. 524-534

[10] Dursunkaya, Z., Keribar, R., and Ganapaty, V., 1994, "*A Model of Piston Secondary Motion and Elastohydrodynamic Skirt Lubrication*," ASME Journal of Tribology, 116, pp. 777-785

[11] Duyar, M. and Dursunkaya, Z., "*Design Improvement of a Compressor Bearing Using an Elastohydrodynamic Lubrication Model*," International Compressor Engineering Conference at Purdue, July 16-19, West Lafayette Indiana, USA, 2002

[12] Greenwood, I. A., and Tripp, J. H., 1971, "*The Contact of Two Nominally Flat Surfaces*," Proc. IMechE., **185**, pp. 625-633

[13] Archard, J. F., 1953, "*Contact and Rubbing Flat Surfaces*," Journal of Applied Physics, **24**, pp. 981-988

[14] Singh, M., Prasad, B. K., Mondal, D. P., and Jha, A. K., 2001, "*Dry Sliding Wear Behavior of an Aluminum Alloy-Granite Particle Composite*," Tribology International, **34**, pp. 557-567

ACKNOWLEDGEMENT

The authors would like to acknowledge Product Development Department of Arçelik A.Ş. Compressor Plant for their support.